Couch-based motion compensation: modelling, simulation and real-time experiments.

Haas, O.C.L. , Skworcow, P. , Paluszczyszyn, D. , Sahih, A. , Ruta, M. and Mills, J.A.

Original citation & hyperlink:
Haas, O.C.L. , Skworcow, P. , Paluszczyszyn, D. , Sahih, A. , Ruta, M. and Mills, J.A. (2012) Couch-based motion compensation: modelling, simulation and real-time experiments. *Physics in medicine and biology*, volume 57 (18): 5787. http://dx.doi.org/10.1088/0031-9155/57/18/5787

Couch based motion compensation: modelling, simulation and real time experiments

Olivier C L Haas[1], Piotr Skworcow[2,3], Daniel Paluszczyszyn[2,3] Abdelhamid Sahih[3] and Mariusz Ruta[1], John A Mills[1],
[1] Control Theory and Applications Centre, Coventry University, Priory Street, Coventry CV1 5FB, UK.
[2]DeMontfort University, Leicester LE1 9BH, UK

E-mail: o.haas@coventry.ac.uk

Abstract. The paper presents a couch based active motion compensation strategy evaluated in simulation and validated experimentally using both a research and a clinical Elekta Precise Table™. The control strategy combines a Kalman filter to predict the surrogate motion used as a reference by a linear model predictive controller with the control action calculation based on estimated position and velocity feedback provided by an observer as well as predicted couch position and velocity using a linearized state space model. An inversion technique is used to compensate for the dead zone nonlinearity. New generic couch models are presented and applied to model the Elekta Precise Table™ dynamics and nonlinearities including dead zone. Couch deflection was measured for different manufacturer and found to be up to 25mm. A feed-forward approach is proposed to compensate for such couch deflection. Simultaneous motion compensation for longitudinal, lateral and vertical motion was evaluated using arbitrary trajectories generated from sensors or loaded from files. Tracking errors were between 0.5 and 2 mm RMS. A dosimetric evaluation of the motion compensation was done using a sinusoidal waveform. No noticeable differences were observed between films obtained for a fixed or motion compensated target. Further dosimetric improvement could be made by combining gating, based on tracking error together with beam on/off time, and PSS compensation.

(Some figures in this article are in colour only in the electronic version)

1. Introduction

Radiotherapy is currently moving from a feed-forward knowledge based approach to an image guided adaptive technique exploiting the feedback from real time imaging and position sensing devices (Verellen *et al* 2008, Krauss *et al* 2011, Murphy *et al* 2008). Treatment can now be individualised in the planning as well as delivery stage by taking into account patient's expected response to treatment and by implementing motion management strategies (Kakar 2010). There is currently a move to reduce the need for restrictive and uncomfortable patient immobilisation methods such as those described in Han *et al* (2011). Robust planning strategies, adopted upstream of treatment delivery, can optimize the treatment based on planning target volume (PTV) taking into account inter and intra fraction patient motion based on the assumption that these are statistically representative (Rijkhorst *et al* 2009). Active breathing requires the patient to follow audio visual instructions (Wong *et al* 1999). Gating waits for the PTV to be in the correct location to irradiate it. It relies on frequent beam starts and stops and can lead to increased session time when the patient cannot maintain regular breathing and the treatment has to be

[3]The work was carried out whilst the authors were at Coventry University, UK

interrupted (Jiang 2006). Multileaf collimators (MLC) track, along two dimensions, either PTV baseline drift (Trofimov *et al* 2008) or shape together with quickly varying motion seen from the beam's source (Keall *et al* 2006). Three dimensional tracking can be achieved by rotating the gantry whilst the MLC is moving, e.g. Elekta Volumetric modulated Arc Therapy (VMAT) (Sun *et al* 2010) and VARIAN RapidArc (Yang *et al* 2011). An alternative is to use, alone or in combination with the MLC, the patient support systems (PSS). Whereas MLC tracks the PTV motion, PSS is moved in the opposite direction to the PTV motion and so immobilise the PTV with respect to the beam. There are three approaches to PSS compensation: i) traditional PSS not specifically designed for motion management (Woo and Kim 2002, D'Souza *et al* 2005, D'Souza and McAvoy 2006, 'Qiu *et al* 2007, D'Souza *et al* 2009, Haas *et al* 2005, Skworcow *et al* 2007, Putra *et al* 2007, Haas *et al* 2011); ii) specifically designed six degrees of freedom robotic table top mounted onto standard PSS, such as the HexaPOD (Wilbert *et al* 2008, Herrmann *et al* 2011) or iii) specifically designed robotic system, such as RoboCouch® which combined with the CyberKnife from Accuray Inc. is still the most accomplished clinical system for motion management (Hoogeman *et al* 2009). Alternatives to traditional gantry designs include ring based machines such as TomoTherapy® (Crijns *et al* 2011, Loo *et al* 2011), VERO (Kamino *et al* 2006) and the Elekta prototype system combining an MRI with a 6MV linac (Crijns *et al* 2011). Each type of equipment and approach has relative advantages and drawbacks identified in the aforementioned citations. A common issue to active motion management is the need to take into account the latency caused by the imaging devices and the communication delays between the various systems that are required to be integrated as well as the seldom mentioned system dynamics that influences the speed of response. The systems latencies are 0.05 s for the VERO (Depuydt *et al* 2011), 0.193 s for the CyberKnife (Hoogeman *et al* 2009) and between 0.160 s (Keall *et al* 2006, Roland *et al* 2010) and 0.4 s (Tacke *et al* 2010) for MLC. The ability of the systems to respond quickly also depends on the maximum available velocity which for PSS compensation has to be limited with the patient's comfort. The maximum achievable velocity are 8mm/s for the HexaPOD (Herrmann *et al* 2011), 30 mm/s for MLC leaves (Popple and Brezovich 2011), 40 mm/s for PSS such as the Elekta Precise Table™ and 60 mm/s for the VERO (Depuydt *et al* 2011). To accommodate the discrepancy between speed of the target and the equipment velocity it is possible to adjust the dose rate (Popple and Brezovich 2011) for MLC and PSS. Similarly dose rate can be adjusted to improve the dose distribution for PSS compensation at a cost of a longer treatment time. This paper considers the need to take into account the time required for the beam to stabilize in order to deliver an accurate number of monitor unit. The proposed method takes into account the current on/off time as well as predicted tracking error and combines it with the current tracking error to decide whether to keep the beam on/off or to switch it off/on. The paper extends the work presented in Haas *et al* (2011) on the use of the Elekta Precise Table™ to compensate for measurable target motion. Experimental results are presented for longitudinal, vertical and when applicable lateral axes. Previously unpublished experimental data on the deflection of Siemens, Varian and Elekta PSS are described and a method to compensate for such deflection is given. The work differs from Buzurovic *et al* (2011b) and Buzurovic *et al* (2011a) in the use of model predictive control (MPC) as opposed to a feed-forward adaptive control or Proportional + Integral + Derivative (PID) control. In Herrmann *et al* (2011) use is also made of MPC where the supervisory controller provides signals to another controller that calculates the acceleration and speed profile to follow. In this work, MPC is able to directly compute the required acceleration and velocity taking into account user selectable limits in terms of both acceleration and velocity. The remainder of the paper is as follows: Section 2 describes the Material and Methods. Section 3 presents the PSS deflection measurements, models, control strategy for motion compensation and the simulated combination of gating and couch based motion compensation. Experimental measurements were carried out on a test system at Elekta, Crawley, UK and a clinical system at the University Hospital Coventry and Warwickshire (UHCW) NHS Trust, Coventry, UK. Section 4 discusses the results and presents the conclusions to the work.

2. Material and Methods

There were multiple components to the overall motion compensation system. The video tracking system detects (using a surrogate marker) the target motion. The overall control scheme calculates the reference required to counteract the target motion. The motion predictor predicts the evolution of the reference. The controller calculates the actions to be done by the PSS to follow the predicted reference

resulting in the PSS following the reference and moving in opposite direction to the target at the appropriate time if the lag equates the prediction horizon. The experimental work was carried out in stages to characterise the Elekta Precise Table™, evaluate the models and assess the compensation strategy. Finally a method exploiting current and predicted compensation errors was used to alter the dose rate, when the errors were above a user defined threshold, to improve the overall dose distribution.

2.1. Video Tracking

A labVIEW video tracking program was developed to detect the motion of two surrogate markers using an IEEE 1394 Foculus digital video camera capable of 30 frames per second with a resolution of 480 by 640. Two algorithms were implemented to track surrogates markers (white disk on a black background) using first pattern matching and then mathematical morphology. The mathematical morphology method involved the following steps: i) detect the markers using thresholding, ii) remove small particles using erosion, iii) identify circular regions of interest with Heywood circularity index, iv) calculate the area of the particles and their centroids, v) reject the small or large objects and check distance between current and previous centroid, vi) convert the pixel positions to the room coordinate system against which the camera was calibrated, vii) record the initial distances between the two markers along the horizontal and vertical directions and use it as reference positions against which subsequent motion are minimized; viii) send the horizontal and vertical distance between the two markers to the motion predictors.

2.2. Experimental set up for the Elekta patient support system

The Elekta Precise Table™ is a 4 degrees of freedom (DOF) manipulator to position patients under the radiation beam. The DOFs are: longitudinal, lateral and vertical and one rotational (around the vertical axis). This work considered the translational DOF. The PSS is equipped with three sets of potentiometers to measure its position along the three translational axes. Each axis comprises one 'coarse' potentiometer to provide a unique position indication for the whole range of motion and two 'fine' potentiometers to provide position information over a significantly smaller range of motion. The 'fine' potentiometers are assembled so as to minimise the effect of the potentiometers' nonlinearity and dead zone. The coarse potentiometers were used to provide position feedback for large position changes. Their resolutions were 104.9, 130.8 and 95.4 mm/V for the longitudinal, the vertical and the lateral axes respectively. One of the 'fine' potentiometer per axis of motion was used to provide position feedback for motion compensation. The reason for using fine potentiometers was the increased resolution and reduced amount of noise compared to the coarse potentiometer. The fine potentiometers resolutions were 7.55, 12.45 and 9.54 mm/V for the longitudinal, the vertical and the lateral axes respectively. To reduce sensors noise both hardware and software low pass filters were implemented. These filters did however add additional lags. The lag increase required an equivalent increase of the prediction horizon to cancel out the overall system lag. Unfortunately increasing the prediction horizon decreases the accuracy of the prediction. A balance had therefore to be found empirically between the amount of filtering, the smoothness of the resulting control signal and the additional system lag. To minimize the amount of modifications to the clinical system and thus possible disruptions in the clinic, a supervisory controller, implemented on a PC based dSPACE 1104 rapid prototyping card (dSPACE), was designed to provide three references directly to the motor drive controllers. Such an approach shortened the development time by letting the manufacturer's software deal with safety issues. Two PSS interfaces were designed. The first interface bypassed the joystick on the PSS and measured the currents directly from the PSS sensors. Similarly to manual control the 'dead man' had to be pressed to enable the PSS to move (Haas 2010a). This ensures that if any issues were encountered the PSS could be stopped immediately. The second method was developed with the support of Elekta and involved direct connection of the PC real time interface with the linac control cabinet. The latter provided a number of benefits linked with the reduced amount of processing done to the signal sent to the PSS drive system and stopped the intervention of the clutch and brakes when the velocity requests were very small. The latter enabled a more reactive controller. It did not, however, reduce the observed system nonlinearities and resulted in an increased dead zone. The initial work on characterisation of the effect of motion prediction on tracking performance was carried out with the first interface and the final demonstration of motion compensation presented in this paper was obtained using the second interface. In both cases good performances were obtained, demonstrating that the algorithms developed could cope with different means of interacting with the Elekta Precise Table™.

2.3. PSS modeling

Model based controllers require a model to calculate the control action. Such a model should be fast to compute and present an acceptable approximation of the actual system. To evaluate the ability of the controller without using the actual PSS, simulation models as accurate as practically possible were developed.

2.3.1. Multi-body mechanical model. A SimMechanics™ model was developed based on the physical characteristics of each DOF of the PSS (Haas *et al* 2005). The mechanical components were represented as rigid bodies. The shape, mass, centres of gravity and inertia tensors of these rigid bodies were defined using information from the manufacturer. The rigid bodies were then linked together using welds, joints and gears. Electromechanical components such as sensors or actuators were interfaced with Simulink™ blocks that modelled the electrical components of the PSS. The actuator inputs represented the drive signals for the motors, which were equivalent to the input voltage that was applied to the PSS. The output signals represented the displacements of the actual axes. The model included some nonlinearities such as friction consisting of static and Coulomb friction, backlash, measurement quantisation and noise, as well as saturation in the voltage input and in the motor torque. The model did not take into account the dead-zone from the electronic interface. Such model was able to replicate the actual system accurately; however they were computationally intensive and required a large amount of information from the manufacturer. Four simplified data based models were subsequently developed.

2.3.2 Linear model. A simplified linear state space model (Linear) was developed to approximate the SimMechanics™ model and be used within the control algorithm to predict the PSS motion. Such model is only valid for a small range of PSS motion. To accommodate for variability in the system it is possible to estimate the model parameters on line and update the model. Such strategy was implemented in simulation; however the experimental results were all obtained using a fixed parameter model. To speed up the simulation studies, simplified data base models were then derived using input-output measurements. The challenge was to estimate the parameters for a representative nonlinear model to relate a velocity request to a resulting position change and be able to replicate the PSS behaviour for typical range of motion as well as velocity and acceleration.

2.3.3 *Asymmetric dead-zone*. The dead-zone is mainly caused by the electronic interface and to some extent to the effect of stiction. It is asymmetric resulting in a constant positive drift. The state space model was combined with the asymmetric dead-zone (Linear+DZ) to improve the model fit. To account for the larger effort required to start the PSS motion than to stop it, a switch friction model (Friction) combining static and coulomb friction was realised.

2.3.4 Nonlinear gain. To model the nonlinear relationship between the velocity request in volt and the actual PSS velocity in mm/s a nonlinear gain (Nonlinear), implemented as a look up table was combined in series with a type 1 second order continuous time transfer function and an asymmetric dead-zone. An alternative discrete time bilinear model (Bilinear) in series with an integrator was implemented to reduce the number of free parameters. Bilinear models are the simplest class of nonlinear systems where the nonlinearity is expressed as a product between the input and output. Bilinear systems are useful to model systems with set point dependent gains such as the PSS where the actual velocity in mm/s does not change linearly with the velocity request in Volt. The difference equation representing the system is:

$$y(k) = -(a_1 - 1)y(k-1) - a_1 y(k-2) + b_0 u(k-1) + \eta_{01} w(k-1)x(k-1) + -\eta_{01} w(k-2)x(k-2) + e(k) - e(k-1) \quad (1)$$

where k is the time in sample, a_1, b_0 and η_{01} are parameters to be estimated with the variable $w(k) = u(k)/(1 - \mathrm{z}^{-1})$ and $w(k-1) = u(k-1)/(k - z^{-1})$ used to account for the need to add a pure integrator in the model to relate velocity request to position. The operator z^{-i} represents the backward shift operator defined by $z^{-i}\, y(k) \equiv y(k\text{-}i)$ with z^{-1} being the unit time delay operator.

2.3.5 Input and output saturation. These nonlinearities are applicable to all models. Input saturations model the PSS velocity limits for each axis. Output saturations model the possible range of motion for each axis.

2.3.6. PSS modelling methodology for data based models. The noise was found to be significant, which explains the presence of a dead zone to prevent the PSS from reacting to noise. The first stage of the modelling process was to remove the noise off line using a median filter to remove the large peaks and then a non causal Chebyshev low pass filter. A noise free signal was then used to model the PSS. The

noise was then modelled as a statistical distribution and implemented in an embedded Matlab® function in Simulink™. The second stage estimated the dead zone which prevents the PSS from moving if the drive signal is below a certain voltage threshold. Positive and negative ramp signals were sent to each axis of the PSS. The voltage thresholds marking the motion start/stop were recorded. The tests were repeated for different PSS velocities (slope of ramp signal), and different load conditions from 0 kg to 70 kg in steps of 13 kg. The next stage was to identify the dynamic response of each axis of the PSS. In addition to the dead zone the friction and stiction influenced the starting and stopping of the PSS axes. It was also found that the gain changed between the velocity request and the measured velocity. Three types of test signals were created and sent to the PSS as velocity requests in open loop. This means that no feedback was used to make sure that the velocity and resulting position changes were following the reference. Step signals for a range of possible velocity requests were used to identify the nonlinear relationship between velocity request in Volt and the PSS velocity in mm/s. These measurements were used to model the nonlinear response as a look up table in the 'Nonlinear' model. Positive and negative ramp signals were sent to evaluate the response of the PSS to constant acceleration. Pseudo random binary sequences were employed to evaluate the response of the PSS to high frequency low amplitude signals. The latter, whilst not representative of patient motion, were used to identify the effect of stiction and friction. To evaluate the ability of the PSS to replicate arbitrary waveforms with varying amplitude and frequency, position signals were differentiated to obtain a velocity request which was then send to the PSS. Assuming that the PSS could behave as a perfect integrator, the resulting measured position should replicate the patient motion signal that was used to deduce the velocity reference. To gauge the likely performances under different load conditions and assess the influence of PSS velocity, acceleration and deflection, the PSS was loaded with a range of masses (40, 68 and 78 kg).
The model parameters for each axis were estimated from measurements using a combination of Nelder-Mead Simplex method implemented within the 'fminsearch' Matlab® routine together with least squares and the genetic algorithms originally used in Haas *et al* (1998).

2.4. PSS deflection. During the MAESTRO project, table top deflections of Siemens (Oncor and Primus), Varian (Clinac 21EX, Clinac 600 C/P) and Elekta (Precise, Synergy) were measured using a Polaris system as an independent measurement device. A LabVIEW interface was designed to perform a coordinate transformation between the Polaris frame of reference and IEC61217. A set of six weight of 13 kg each were successively added, starting from the end of the table top, along the table top centre line along the longitudinal direction of motion. The maximum load was 78 kg. The table top was then moved from/to its resting position to/from a fully extended position, whilst the Polaris™ recorded the spatial position of a standard tool. The deflections observed, at specific longitudinal positions, during the forward and reverse motion were then averaged and stored in a look up table. The look up table was then used by the control system during the initial positioning phases to automatically increase the vertical position based on the longitudinal position of the table top and the load, thereby compensating for the sag of the table top. Two methods were used to evaluate the effect of deflections in terms of angular change along the longitudinal direction. The first method involved comparing the Polaris tool orientation with and without load. The second method uses trigonometry to deduce the angle of the table top based on the deflection and assuming a field size of 200 mm by 200 mm such that: $\phi_{Deflection}=\tan^{-1}((D_{900}-D_{700})/(900-700)$ where D_{900} and D_{700} indicate the deflection measured at longitudinal position 900 mm and 700 mm respectively. To assess the hysteresis, the data corresponding to the forward and reverse motion were fitted with polynomials to provide smoothed approximation of the trajectories. The distances between the two trajectories were then calculated using the smoothed trajectory every 0.1 mm increment from 0 to 900 mm for the Siemens PSS, from 0 to 1000 mm for Elekta PSS and from 0 to 1200 mm for Varian PSS.

2.5. Motion prediction
A constant velocity Kalman filter developed by Putra *et al* (2008) and adapted for real time implementation was used as a compromise solution in terms of accuracy of surrogate motion prediction and computational complexity. To avoid prediction errors from one axis to impact on prediction error on other axis of motion and enable slightly different tuning of the predictor for the different axes, three constant velocity KF predictors were implemented, one per axis of motion. Predictors used in the literature, see for example (Ernst *et al* 2011, Murphy and Pokhrel 2009) and references therein,

calculate only a single prediction that is then used by a traditional controller. The adoption of model predictive control provides the mean for the controller to consider a range of predicted positions to calculate the most appropriate control action. The constant velocity KF is used to predict positions from the current time or from time H_L to time $H_L + H_u$ where H_L is the system latency and H_u the control horizon. The prediction horizon $H_L + H_u$ to overcome the latency was determined from experiments and depended on the set up. The prediction horizon $H_L + H_u$ used were in the range [17, 24] samples or [0.34, 0.44] s in the case where the reference to be followed was provided by a file or a motion sensor and [0.56, 0.70] s where the reference was provided by video tracking. In the case of the dosimetric evaluation of 2D motion compensation, see Sections 2.7 and 3.3, $H_L + H_u = 18 + 10 = 28$ samples or 0.36 + 0.2 = 0.56s.

2.6. Control system development

The control system development was implemented in stages. Initially a PID was used as a benchmark. PID can react to current error using the proportional action, correct for ongoing errors using the integral action and correct for short term predicted errors using the derivative action. The PID controller was combined with a feedforward prediction using either the Kalman Filter or a PD controller using the derivative control action to compensate the system latency. A Smith predictor combined with a PID was also investigated to accommodate for system lag due to dynamics as well as output delays. The proposed constrained model predictive controller was implemented to exploit the systems dynamic response prediction as well as the predicted target motion to calculate the current control action $u(k)$. Constraints were imposed on the maximum PSS velocity and torque to ensure that the motion requested by the controller was comfortable and within the operating limits. The velocity constraints were:

$$V_{min} \leq u(k) \leq V_{max}$$

where V_{min} and V_{max} correspond to the minimum and maximum drive voltage magnitudes that should not be exceeded by the control action $u(k)$, with k is the time in sample, to make the PSS move in one direction or its opposite. Using the first set up V_{min} = 3 V and V_{max} = 7 V with 5 V representing the output voltage sent if the velocity request was null. In the second set up V_{min} =-2 V and V_{max} = 2 V. The motor torque constraints T_{max} were expressed as follows:

$$-T_{max} \leq \theta_1(\theta_2 u(k) - \theta_3 \dot{y}(k)) \leq T_{max}$$

where $\dot{y}(k)$ denotes PSS velocity, and θ_1, θ_2, θ_3 are constants of the motor-gearbox mechanism. At each sample step k the Kalman filter predictor calculates the motion from k+1 *to* $k+H_L+H_p$ but only sends to the MPC controller the predictions H_L to $H_L + H_p$ in a vector of predicted target positions, denoted $\hat{Z} = [\hat{z}(k + H_L \mid k),.., \hat{z}(k + H_L + i \mid k),.., \hat{z}(k+H_L + H_p \mid k)]$. The notation $\hat{z}(k + H_L \mid k)$ refers to the estimated prediction made at time k for the time $k+H_L$ in the future. The MPC control action is calculated by minimising, using quadratic programming, the weighted sum $J(k)$ between the predicted tracking error and the future control actions:

$$J(k) = \sum_{i=1}^{H_u} \|\hat{y}(k + H_L + i|k) - \hat{z}(k + H_L + i|k)\|^2_{Q(i)} + \|\Delta\hat{u}(k + H_L + i - 1|k)\|^2_{R(i)}$$

where $\hat{y}$ and $\hat{u}$ are predicted output and input, respectively, $\Delta = 1 - z^{-1}$, $Q(i) \geq 0$ and $R(i) > 0$ are controller weight, H_p is the prediction horizon $H_u = H_p$. MPC uses the vector of prediction $\hat{Z}$ as a reference trajectory to calculate, using its internal model, what would happen if the sequence of control action $[\hat{u}(k+H_L \mid k), .., \hat{u}(k+H_L + i \mid k),.., \hat{u}(k+H_L + H_u \mid k)]$ were to be applied to track the reference. A receding horizon strategy was adopted to calculate the one step ahead prediction of the PSS output $\hat{y}(k+H_L+1|k)$ where only the first input $\hat{u}(k+H_L \mid k)$ from the optimal input sequence is used to calculate the incremental control action $\Delta\hat{u}(k+H_L \mid k+H_L)$ to add to the current control $u(k-1+H_L)$. The ratio $Q(i)/R(i)$ weights the relative importance of accurate motion tracking or compensation and smooth control action for a comfortable ride. In Skworcow *et al* (2007) it was shown, using simulation studies, that adjusting the $Q(i)/R(i)$ ration as a function of the expected prediction error was beneficial. During the real time experiments, to reduce the overall system complexity, $Q(i) = Q$ and $R(i) = R$ were set as constants scalars selected empirically to achieve an acceptable trade off between accurate compensation that could lead to very active controller resulting in 'shaky' motion and a smoother 'ride' for the patient at the cost of a decreased compensation accuracy. Note that the PSS acts as a low pass filter which had the positive effect of filtering out some of the high frequency changes in the control action making them invisible to the PSS position sensors. Readers interested in a more detailed formulation of the MPC controller should refer to Skworcow (2008) and Maciejowski (2002).

To cope with the nonlinearities, the real time hardware implementation required the use of a compensator which was selected as the inverse model of the nonlinearities. Such compensator aimed to cancel out, from the controller's perspective, the effect of the asymmetrical dead zone and part of the nonlinear system gain enabling a linear controller to control a nonlinear system by making the combination of compensator together with the nonlinear plant appear linear. The compensated control action u_c was calculated as follows:

$$\begin{aligned} &\text{if } u(k) > +u_{SmallOffset}, && u_c(k) = f_{pos}(u(k))^* u(k) + u_{PosOffset} \\ &\text{if } u(k) < -u_{SmallOffset}, && u_c(k) = f_{neg}(u(k))^* u(k) - u_{NegOffset} \\ &\text{else} && u_c(k) = 0 \end{aligned}$$

where $u_{PosOffset}$ and $u_{NegOffset}$ are deduced from measurement and subsequently tuned by the system identification software developed to cancel the drift observed during the open loop tests. $u_{SmallOffset}$ is a small positive number, an order of magnitude smaller than the existing dead zone, aimed to create a small symmetrical dead zone which function is to prevent the control action from changing based on very small tracking errors. In most of the experimental work $f_{pos}(u(k))$ and $f_{neg}(u(k))$ were selected to be one or two constant gains. Note that small model matching improvements can be obtained by varying these aforementioned functions as functions of the PSS velocity.

2.7. Overall system implementation

The overall system comprises a constrained MPC (Skworcow 2008), a constant velocity Kalman filter prediction algorithm (Putra *et al* 2008), a PSS nonlinearities compensator and an observer to provide estimates of the PSS position and velocity based solely on position measurements. Matlab® and Simulink® (MathWorks 2011) were used to implement the control algorithms, with the real time workshop toolbox employed to convert the Simulink®, Matlab® and C code to a real time C code that was executed on the dSPACE real time hardware. The constrained MPC and Kalman predictor were implemented in C to enable the user to interact with their tuning parameters online through the dSPACE ControlDesk user interface. To reduce interactions between the controllers it was decided to implement three independent predictor + observer + controllers + compensator, i.e. one per axis. A look up table was used to compensate for the PSS table top vertical deflection by automatically increasing the vertical position based on the position of the table top in the longitudinal direction. Note that the deflection compensation was switched off during the tracking and compensation as the differences in table top deflection were negligible over displacements in the range of 0.1 m about a given location. The simulations used either the SimMechanics model or the continuous time type 1 second order system with dead zone and saturation. Controller tuning was performed off line based on simulation models of the PSS and using Nelder-Mead Simplex Method implemented within the Matlab® fminsearch routine.

2.8. Experimental validation of PSS positioning, tracking and compensation

The initial work involved the validation of the PSS model used as a basis for the controllers' development. The second stage of the work evaluated the ability of the PSS to move to and from a number of set positions. The third stage focused on the tracking ability of the new control scheme. Position requests were sent to the supervisory controller which calculated the required trajectory. The controller was demonstrated on the clinical system at UHCW as well as on a test system at Elekta Crawley, UK highlighting that it could be adapted to different hardware set up. The experiments carried out at Elekta, UK involved generating a square wave with the range of period (2 to 7 s) and amplitude (6 to 18 mm) observed in George *et al* (2005) and then using it as an input to drive a bilinear model to generate a test sequence representative of external motion (Sahih 2010). Having demonstrated that the controller was able to follow one-dimensional (1D) irregular motion trajectories for different PSS configurations, the next stage was to evaluate the 1D and then three-dimensional (3D) response of the system to position requests sent by a position sensor. This stage was introduced to evaluate the control system response under the most favourable circumstances where the sensor noise was negligible and the lag between the position measurement and the PSS reaction minimal. The sensor was initially moved by hand over a range of 50mm combining slow as well as fast variations. Initially a single axis was controlled see (Haas 2010a). Subsequently, the same signal was sent to all three axes, see Section 3.3.1. Having demonstrated that the PSS was able to respond to position requests sent from a position sensor actuated manually, the next stage was to introduce video feedback. The latter introduced a new lag due to different sampling times between the controller and the video tracking system and increased the

complexity associated with tuning the Kalman filter motion predictor as well as the MPC controller. Finally a dosimetric evaluation of 2D motion compensation using the MAESTRO phantom (Haas *et al* 2011) was performed to validate the overall approach (Haas 2010b).

2.9 Gating combined with PSS compensation. Two methods were investigated to decide the switching of the beam on and off depending on the tracking/compensation error. First only the current tracking error was used. If both longitudinal and lateral errors were above/below a user selectable threshold the beam was assumed to be off/on. The second method was refined by taking into account a predicted error calculated by fitting a second order polynomial or order $n \in [1, 3]$ to the last $n_{Past} \in [10, 40]$ samples to predict the next $n_{Future} \in [10, 20]$ samples with a sampling time of $T_s = 0.05$ s. The predictions were used to keep the beam on/off in cases where they were above/below the threshold and the beam had previously been on/off respectively for a user selectable period of time. The PSS velocity was monitored to identify a link between tracking error and target velocity. The simulated irradiation method developed in Haas *et al* (2011) was used to evaluate the effect on the resulting dose distribution of applying gating based on the tracking error. Thresholds between 0.5 and 2.5 mm were investigated. A small threshold would lead to frequent dose rate changes which would negatively impact on the components lifetime. In the trajectory used for the 2D motion compensation of the MAESTRO phantom motion a threshold of 1 mm was found to be suitable.

2.10. Performance indicators

To evaluate the feasibility of motion compensation using a standard Elekta PSS, criteria based on the positioning accuracy as well as on simulated and actual radiation delivered were adopted. To evaluate the tracking accuracy in mm, the root mean square error (RMSE) between the reference and the actual PSS position recorded both by the PSS sensor and by an independent measurement device (namely a camera) was calculated. The performance of the control system should be evaluated not only in terms of the resulting tracking error and amount of energy used to reach the desired trajectory but also in the manner with which such performance is achieved. Therefore the criteria adopted emphasise the importance of limiting the change in control action between two successive samples such that $C_{ctrl} = \sum_{k=1}^{n} |u(k) - u(k-1)| / n$ where n is the number of samples. The final experiment performed for the MAESTRO project involved the irradiation of three films. The first was irradiated with a fixed target and constituted the gold standard. The second was irradiated with the target moved according to a sinusoidal waveform during the irradiation. The third was irradiated with a moving target whose motion was compensated by the PSS to attempt to immobilise it with respect to the beam.

3. Results

3.1. PSS modelling

The PSS models presented in Section 2.3 were implemented in Simulink, see figures 1 to 3. The blocks highlighted represent the nonlinearities modelled in each system. The saturation and dead zone are common. The input saturation block limits the maximum voltage used to move the PSS. The output saturation limits the possible displacement of the PSS along each axis of motion. Other blocks presents in figures 1 and 3 include triangular blocks which are gains. Square blocks with a '0' are constants representing initial conditions, square blocks with '1/s' represent integrators in the continuous time domain, square blocks with 1/z represent unit delays used to implement the backward shift *k*-1 and *k*-2 in (1), Section 2.3. The signal used as an input in figure 4 was obtained from an external motion trajectory as follows: the derivative of the signal, denoted 'ideal', was calculated and a dead zone compensation of the order of +/-1.6V was applied to artificially increase the drive voltage above to enable the PSS to move. Due to all of the PSS nonlinearities not being accounted for and the system not being controlled, the resulting trajectories were, as expected, not identical to the trajectory denoted 'ideal'. The observed upwards drift was due to stiction, friction and the electronic interface resulting in an asymmetric dead zone with different lower and upper limits. These limits vary slightly to account for the effect of friction directly or indirectly within the models. Identifying the model parameters leads to very similar performances for all the models, the most important factor being the dead zone, see figure 4. The linear state space model, denoted 'Linear', without dead zone is, as expected, only able to fit part of the system. The best model fit with the measured PSS position, denoted 'Sensor', was obtained using

the bilinear model (figure 3), denoted 'Bilinear' in figure 4, RMSE= 0.98 mm, followed by the model with a look up table to model the nonlinear gain (figure 1), denoted 'Nonlinear' in figure 4, RMSE=1.21 mm and the 'Friction' model (figure 2) RMSE = 1.43 mm. Such accuracy is believed to be sufficient from a simulation perspective.

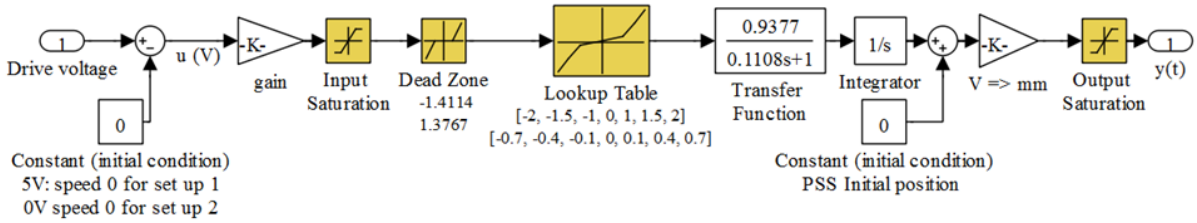

Figure 1. Continuous time (s notation) model combining in series a type one system composed of a linear transfer function with a gain equal to 0.9377 and a time constant T= 0.1108s with a pure integrator. The nonlinear elements include an input saturation, a dead zone between -1.4114 V and 1.3767 V, a look up table representing the nonlinear response of the table to the drive signals and an output saturation to represent the limits of the range of motion. The constant gains are used to improve the model fit or perform the conversion from volt and to mm. Constants, set to 0 in this example, are used to initialise the model for a particular set of initial conditions.

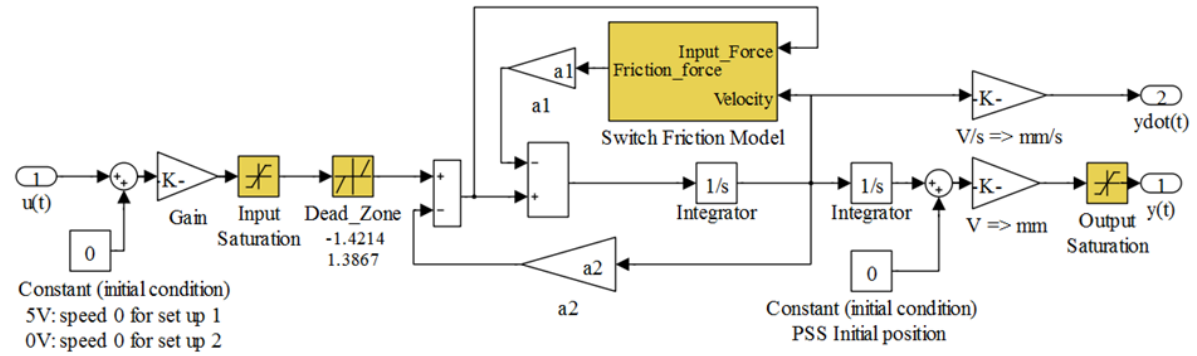

Figure 2. Continuous time (s notation) model combining a linear second order system implemented using two pure integrators (1/s) and with the gains a1, a2 which combined with the nonlinear switched friction model relate to the dynamic response of the system. The implementation of the second order transfer function as two integrators is used to enable to input the modelled velocity as well as the input force into the switched friction model.

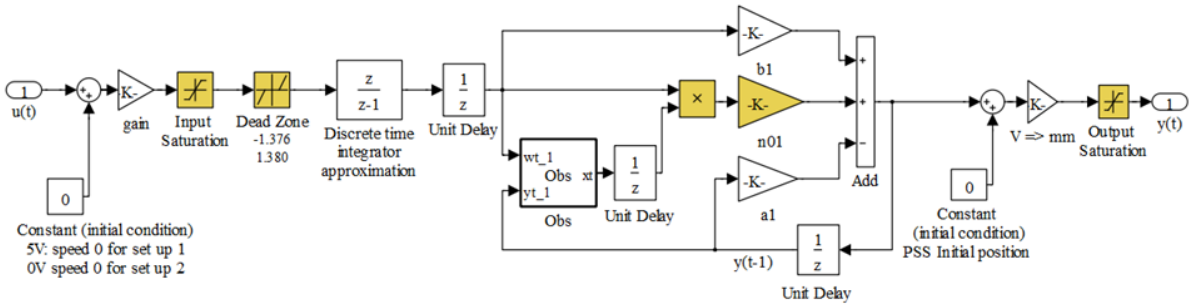

Figure 3. Discrete time (z notation) bilinear model of the PSS replacing the look up table in figure 1 by the product (represented by the square block with x) between the PSS output position estimated through an observer (Obs) and the input creating an input dependent gain. The 1/z blocks represent unit delays employed to implement the time shift in the difference equation (1), Section 2.3.

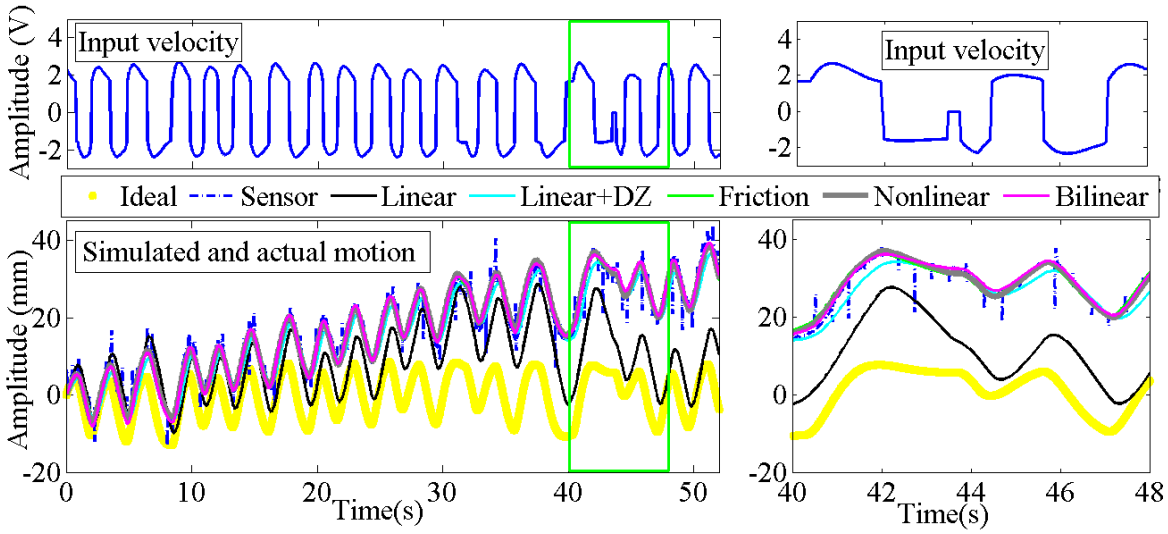

Figure 4. (Bottom) Comparison between the different model responses denoted 'Linear', 'Linear+DZ', 'Friction', 'Nonlinear' and 'Bilinear' see Section 2.3 to a statistically representative marker trajectory, denoted 'Ideal' (bottom). This 'Ideal' signal was differentiated and an approximate dead zone compensation applied to create the Input velocity signal (top) applied to the models developed in Section 2.3. The most significant factor is the dead zone modelling followed by the nonlinear relationship between the motor drive input voltage and the PSS velocity. The linear state space model is therefore sufficient for using within the MPC as long as the dead zone is accommodated for using the implemented inversion technique.

3.2. Deflection compensation

The evaluation of table top deflection at four UK sites highlighted that it should be accommodated by the control system during the initial positioning stage; however it is not considered to be significant when using a PSS for motion compensation. The maximum PSS deflection was 10, 25, 13 and 14 mm for Siemens Primus, Siemens Oncor (figure 5), Elekta and Varian table tops respectively. The Siemens Oncor had the longest unsupported table top which, despite its carbon fibre built, caused the largest sag. Hysteresis was present, with the maximum discrepancy between the forward and backward motion being less than 0.2, 0.4, 0.3, 0.1 mm for Siemens Primus, Siemens Oncor, Elekta Precise and Varian table top respectively. The hysteresis increased only marginally with load: less than 0.1 mm for Varian and Siemens Primus, and about 0.1 mm for the Siemens Oncor and Elekta. The Elekta table top used in this work was found to deflect by a maximum of 12.82 mm for a load of 78 kg. These measurements were then implemented in a look up table such that when the PSS table top moved along the longitudinal direction and extended forward, the vertical position of the PSS was automatically increased. Note that such an approach does not account for the bending of the table top which results in a small change of angle of the table top as well as a change in vertical position. The angle of the table top was estimated at 0.3 degree assuming a 14 mm deflection and 0.9 degree for a 25 mm deflection. Figure 6 illustrates the programmed vertical increase by 7 mm of the reference position as a function of the longitudinal position. The control action makes the PSS move as fast as possible (+2 V) in the longitudinal direction and concurrently performs small adjustments (+0.5V) to the PSS vertical position to compensate for the expected sag for a mass of 39kg.

a) 

b) 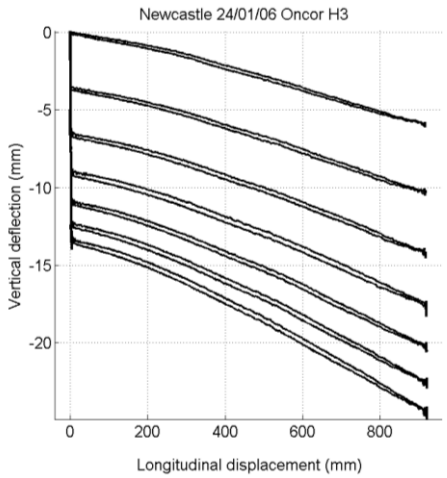

Figure 5. Siemens Oncor Table top deflection: a) set up showing tool tracked by Polaris^{TM} positioned next to three weights, representing a total mass of 39 kg. b) Trajectories followed by the tool tracked by the Polaris^{TM} for 0 kg (top trajectory), 13 kg, 26 kg, 39 kg (4th trajectory from the top), 52 kg, 65 kg and 78 kg (bottom trajectory) highlighting significant deflection, some hysteresis and table top oscillation when reaching the end position.

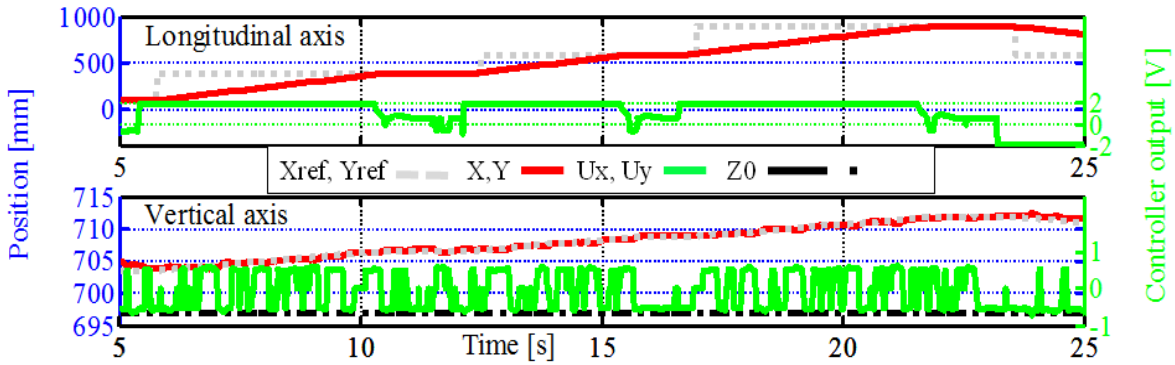

Figure 6. Illustrating the deflection compensation based on measured deflection for different PSS positions along the longitudinal axis. (Top) represents the successive step changes requested 'Xref' and the measured longitudinal PSS position 'X'. The control request 'Ux' makes the PSS move at constant velocity (X increases in a straight line before reaching the reference position) before stopping when the 'Xref' is reached. (Bottom) represents the vertical reference 'Yref' calculated to compensate for the PSS deflection by lifting the table top. It results in a steady increase of the vertical position 'Y' caused by the control action 'Uy' calculated to make 'Y' follow 'Yref'. The vertical PSS position for a load of 0kg is represented by 'Z0'. It shows the PSS deflection for a load of 39kg increasing from 9 mm to 16 mm, see figure 5.

3.3. Position tracking

Haas (2010a) shows the progression of the experimental work from controlling a single axis at a time to controlling each translational axis independently based on a reference provided by a position sensor to simultaneously controlling the longitudinal and lateral axes from signals read from files.

3.3.1 Simultaneous tracking (3D) of position reference from sensor (clinical PSS). Figure 7 illustrates the concurrent control of three axes from a reference obtained from a motion sensor. It demonstrates that similar performance can be achieved for all three axes when tracking arbitrary trajectories. RMSE of the order of 0.4 and 1.5 mm were observed depending on the trajectories. The most significant factors were the identification of the prediction horizon and the Q/R ration. Note that the inversion method to cancel the dead-zone can lead, as expected, to unwanted rapid changes in control action at low velocity.

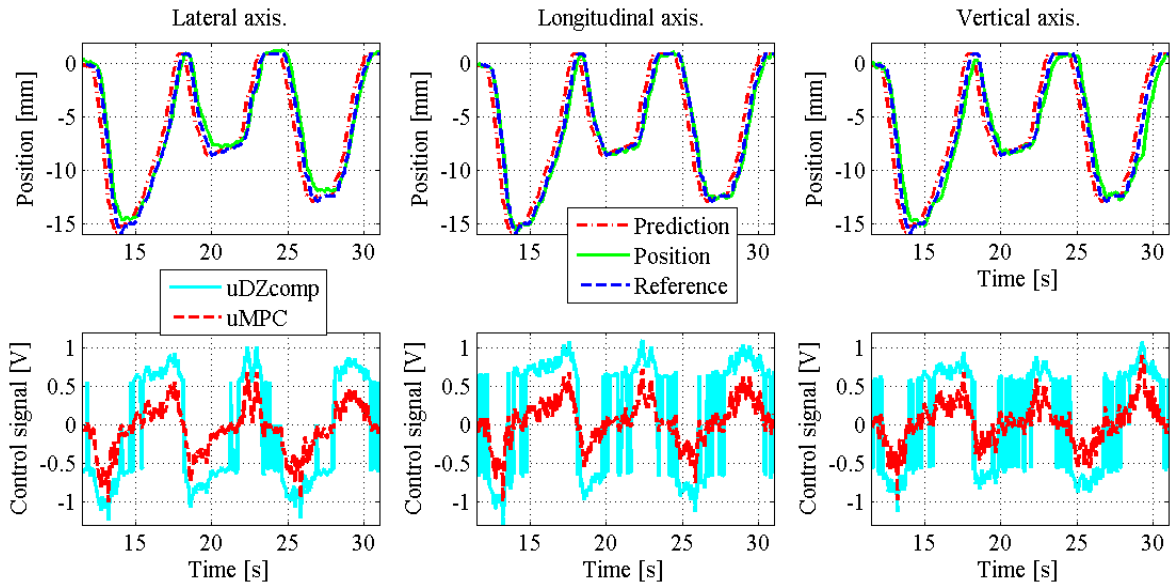

Figure 7. The controller moves simultaneously the three translational axes to follow an identical trajectory provided by a position sensor (Haas 2010a); RMSE [mm]: 0.72, 0.44, 1.04 and C_{Ctrl} = 0.034, 0.043, 0.046 for the lateral, longitudinal, and vertical portion of the Lateral, longitudinal and vertical axes. PSS maximum |velocity| = 16 mm/s, mean |velocity| = 4 mm/s.

3.3.2 Tracking (longitudinal) of motion trajectory generated by a bilinear filter (research PSS). The predictor leads to RMSE of 1 to 2 mm for a prediction horizon of 0.3s required to compensate the system lag, see figure 8. The maximum velocity of the PSS (40 mm/s) during this test was significantly higher than figure 7 resulting in higher control efforts. The constant velocity KF was found to overshoots when the motion changes direction. This behaviour was exploited by adopting a Q/R ratio that focused on producing a smooth action by contrast to fast and accurate tracking. Adopting a joint predictor-controller tuning approach leads to good tracking performance (RMSE < 0.5 mm) and a smoother control action compared to that in Figure 7.

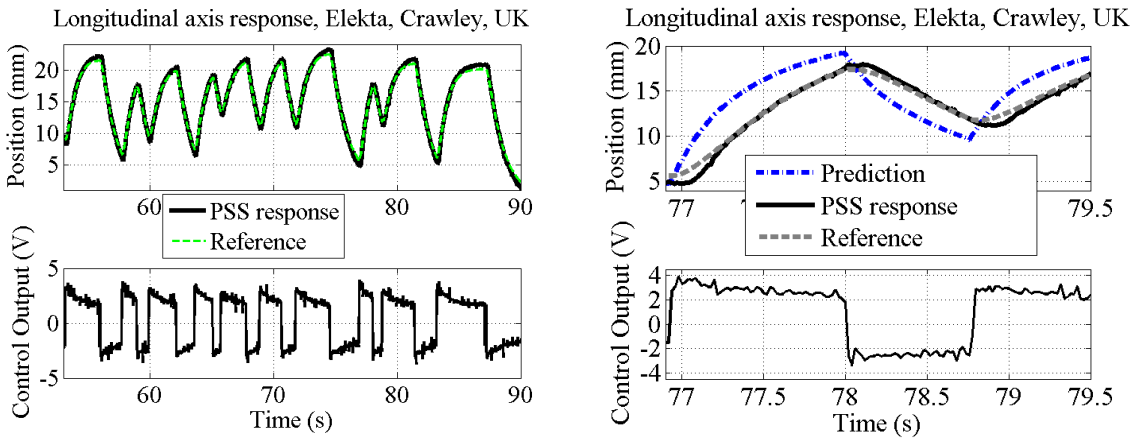

a) Trajectory with varying amplitude and period

b) Tracking over a period of 2.5s

Figure 8. Illustrates the ability of the control system to make the PSS follow an arbitrary trajectory sent to the control system directly from a file; a) illustrates the controller response (bottom) to the changes in period and amplitude of the trajectory(top); b) subset of a) to visualise the 0.3s ahead prediction able to compensate all systems lags resulting in very accurate tracking with RMSE [mm] a) 0.5, b) 0.53 with C_{Ctrl} a) 0.27, b) 0.35 and PSS maximum |velocity| =40mm/s, mean |velocity| =8 mm/s.

3.3.3 Dosimetric evaluation (2D), sinusoidal waveform: 12 mm peak to peak amplitude, period 6.2 s. Experimental set up and resulting dose distributions captured by three films and surrogate marker

motion trajectories for the vertical and longitudinal axes of motion are illustrated in figure 9 and described in details in Haas (2010b). The dosimetric comparison indicates that uncompensated motion of a circular target leads to under dosing of the target along the direction of motion (diagonal) but also perpendicular to it. RMSE, see Table 1, of the order of 1 mm are observed in the best case (Zones 1, 3 and 5) and up to 2 mm when loss of markers occurs (Zone 2). The tracking performance of the PC based LabVIEW tracking system was one of the bottlenecks of the work. The pattern matching was slightly more robust but resulted in smaller number of measurements per second. The loss of targets by the video tracking system was due to different lighting conditions between the research lab and the linac bunker as well as on the motion of human observers around the room. In case of loss of tracking it was decided to use the last known good position given that the motion predictor implemented within the control system could overcome some of this loss of tracking for short time duration. The observed tracking errors were not significant from a dosimetric perspective with the static and motion compensated films being almost identical with the exception of a slight blurring of the edge of the motion compensated film, see figure 9.

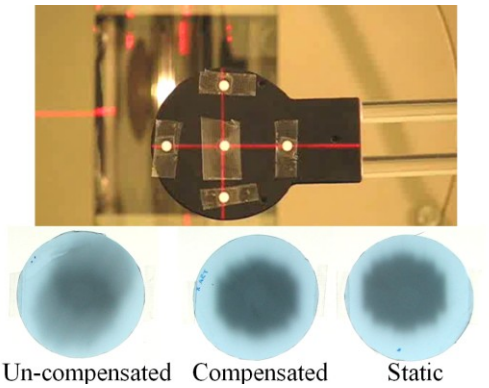

a) Film irradiation set up

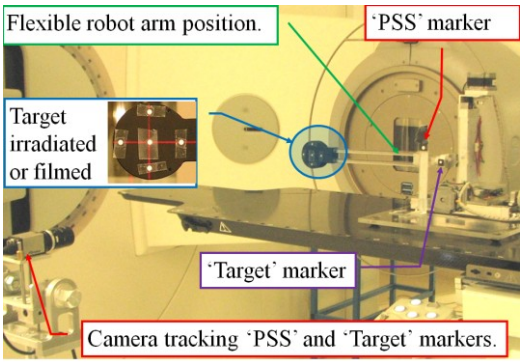

b) Overall PSS compensation set up

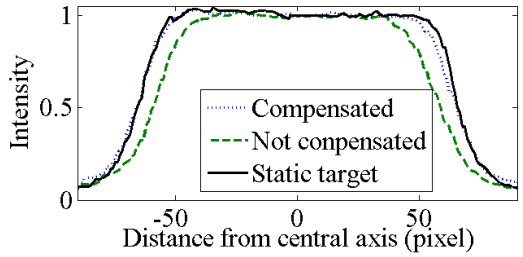

c) Dose profiles perpendicular to motion direction

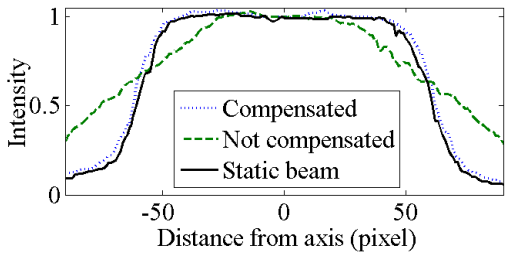

d) Dose profiles along direction of motion

Figure 9. a)* and b) film holder (top) located at the end of a flexible robotic arm part of the MAESTRO phantom (Haas, 2010a, 2010b). The 'Target' and 'PSS' markers are mechanically linked to the film holder and the PSS table top respectively. The white circles have a diameter of 2.5 mm. The three films correspond to non compensated 2-dimensional motion (left) PSS compensated motion (middle) and static field with a static target (right). Dose profiles perpendicular (c) and along (d) direction of motion. *Reprinted from Proc. 18th IFAC World Congress Milan, Italy 2011.

Figure 10 shows the idealised 'Phantom' trajectory that should be compensated by the PSS to keep the 'Target' immobile with respect to the treatment beam. This should be realised by imparting to the 'PSS' a motion in opposite direction to that of the 'Phantom', thereby 'compensating the phantom motion. In practice, compensation errors result in a residual target motion 'Target' measured using the surrogate marker physically connected to the film holder representing the target to be irradiated (figure 9b). The residual target motion is identical to the 'Phantom' trajectory when the compensation stops (zone 4, Table 1 and between 104 and 130 s in figure 10). In other zones the errors oscillate between +/- 2 mm and +/- 5 mm, see MAX error in Table 1. The large errors occurred in general at high velocities, when the PSS trajectory crosses zero. This indicated that the prediction horizon of the order of 0.56s did not compensate for the whole system lag and latency. Subsequent analysis of the results, see figure 11,

indicated that in addition to the modelled system latency H_L = 0.36s (lag between the dotted line 'Prediction' and the dashed line 'Position'), an additional latency of 0.08s was present between the 'Reference' (plain black line) and the PSS output ('Position' or 'Sensor reading'). The control horizon of 0.2 s (Section 2.5) aimed to anticipate the dynamic response of the PSS and did not compensate for the mismatch between the system and the modelled latency. Note that to facilitate the qualitative evaluation of the performance of the control scheme and identify the aforementioned un-modelled lag, the reference, the prediction and the PSS trajectories in figure 10 were negated to form the trajectories displayed in figure 11. Using such a transformation, the ideal compensation should result in superimposed trajectory as opposed to symmetrical trajectories. In practice, the position given by the camera is negated to provide a reference that would result in PSS motion being exactly opposite to that of the target in order to keep the target still with respect to the treatment beam. Simply following this 'Reference' would lead to the PSS trajectory consistently lagging H_L samples behind the 'Reference'. The reference is therefore used by the predictor to generate the trajectory 'Prediction' leading by H_L samples the trajectory that should be followed by the PSS ('Position' or 'Sensor reading').

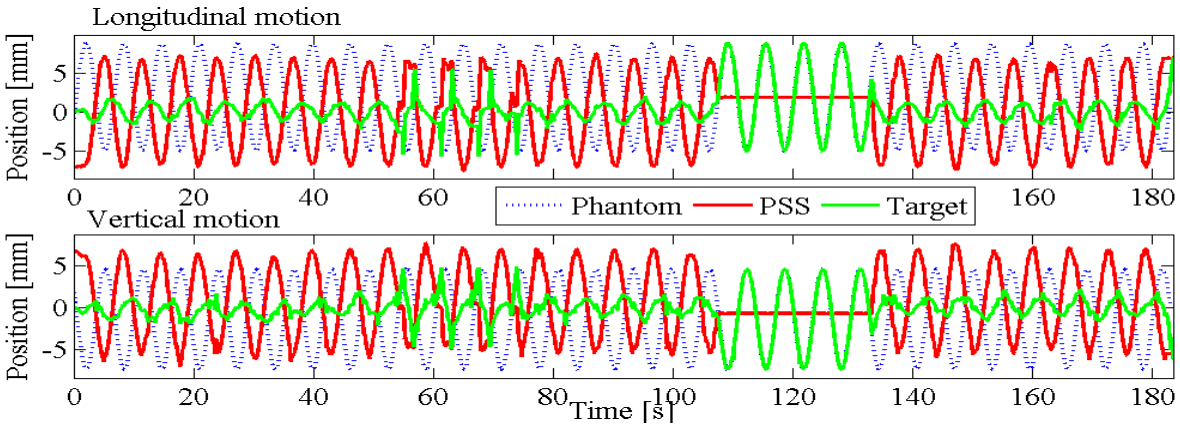

Figure 10. Longitudinal and vertical 'PSS' position and 'Target' position (residual error) seen by the camera combined with the reconstructed 'Phantom' trajectory to visualise the PSS motion which should be opposite to the phantom motion. Errors and Control cost are in Table 1.

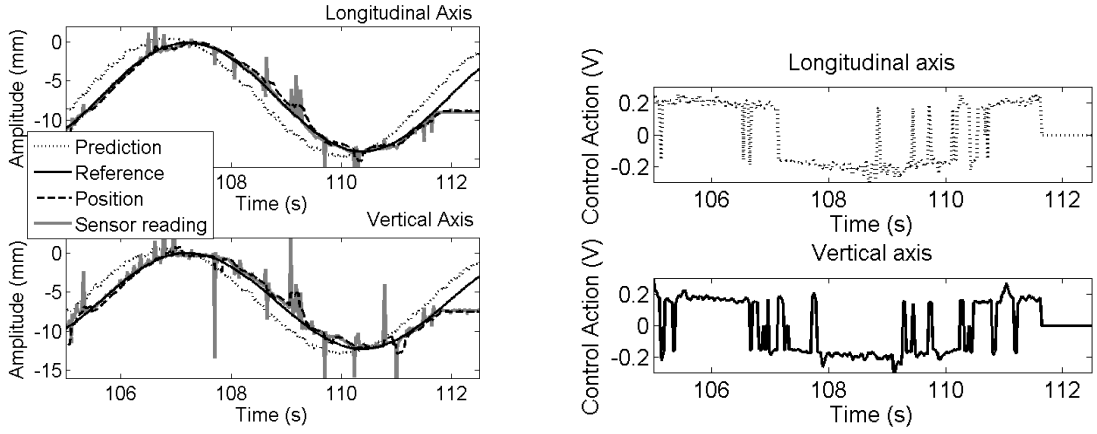

a) b)

Figure 11. Represents a small time interval from figure 10 seen by the control system; a) represents the desired trajectory 'Reference' to be followed by the PSS which position is measured by a potentiometer 'Sensor reading' and filtered to give the 'Position' signal used by the controller to calculate its next control action b). The presence of lag means that to follow the 'Reference' it is necessary to anticipate it such that the 'Prediction' becomes the desired trajectory, 0.4s ahead of the 'Reference'. The controller will aim to follow the 'Prediction' in order to make the PSS actually follow the 'Reference' (C_{Ctrl} = 0.3). The errors between the reference and the PSS position (RMSE of 1.47 and 1.23 mm for the longitudinal and vertical directions) give rise to the residual target motion observed in Figure 10. It is due to a small un-modelled lag of 0.08s which can be observed between the 'Reference' and PSS 'Position'.

Table 1. Residual target motion (Error) and control effort C_{Ctrl} for the longitudinal (Long) and Vertical (Vert) directions, over 5 zones (corresponding to the time intervals ΔT in Figure 10) exhibiting Normal performances, performance affected by video tracking issues (Marker loss) and a zone when the compensation was not active (Off).

Zones	1: Normal		2: Marker loss		3: Normal		4: Off		5 Normal	
ΔT [s]	0 - 45		45 - 73		73 - 104		104 - 130		130 - 174	
Error	Long	Vert	Long	Vert	Long	Vert	Long	Vert	Long	Vert
Mean	0.15	-0.31	-0.17	-0.02	0.00	0.00	1.93	-1.40	-0.02	0.09
RMSE	0.96	0.88	1.74	1.77	0.94	0.81	5.21	4.46	1.03	0.93
CI 95	2.01	1.93	3.56	3.48	1.85	1.59	11.42	9.71	2.03	1.91
MAX	2.12	2.07	5.58	4.93	2.07	2.07	8.91	7.46	3.89	2.87
C_{Ctrl}	0.26	0.37	0.36	0.56	0.27	0.42	0.00	0.00	0.33	0.34

3.4 PSS compensation combined with dose rate variation or gating

The simulated dose rate variation was found to be able to reduce the dosimetric error due to compensating errors above a user defined threshold but at the cost of a longer irradiation time and increase treatment complexity and associated risks with changing the dose rate repetitively. Figure 12 compares two gating techniques combined with PSS compensation. The first assumes that as soon as both position errors are below 1 mm the beam can be on. The second strategy attempts to minimise switching the beam on/off and off/on for short durations by exploiting the predicted error and the current beam on or beam off time. Such approach keeps the beam off even if the error is within limit for short period of time e.g. at times between 110 s and 140 s in figure 11a and at time 55 s in figure 12b-d. A drawback is that it delays the switching on of the beam between 40 and 45 s in figure 12b-d following a period where the beam was off. Figures 12 e-g show that both strategies are similar from a simulated dosimetric view point with the advantage that, in most cases, the proposed strategy 'Beam On 1' can reduce the occurrence of short beam on/off time. The non uniformity in 12e is due to the uncompensated target motion between time 108 and 133s in zone 4 (see figures 10 and 12a). The challenge is similar to that of motion prediction in that such scheme relies on an accurate ability to predict the evolution of the error. It is often the case that large compensation errors correspond to large PSS velocity. The use of velocity to predict switching of beam is however difficult due to noise. An alternative could be to use the predicted target or PSS position.

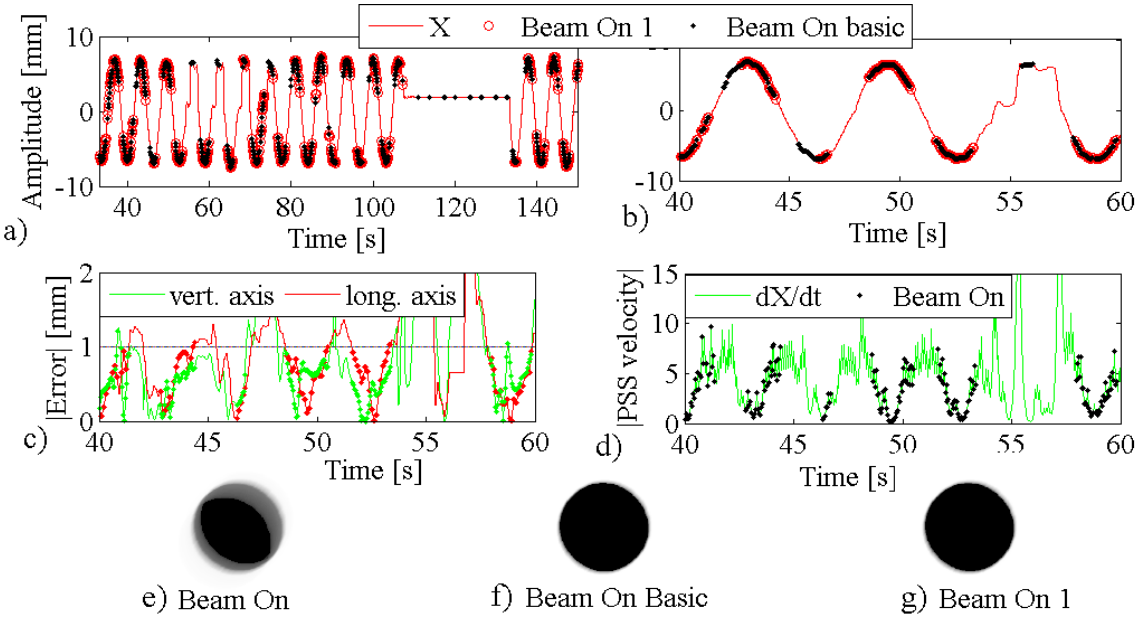

Figure 12. a) Illustrates the PSS trajectory along the longitudinal direction. A zoomed version of a) is presented in b) with the corresponding tracking error for both longitudinal and vertical axes in c) and the PSS velocity which is correlated to the target velocity in d). The dots in c) and d) indicate the beam on time according to the method proposed in Section 2.8. The resulting simulated irradiation are in e) to g).

4. Conclusions

This paper has shown that widely available patient support systems can still be used as a method for translational motion management. All the PSS evaluated in this study used a cantilever design and as a consequence suffered from significant deflection depending on the mass located onto it. Such deflection was found to be of importance for the initial positioning phase but was not critical for motion compensation where the range of motion is likely to be less than 100mm. Whilst PSS such as the one within the Elekta Synergy treatment suite were not designed for motion compensation, they can prove a cost effective alternative to highly accurate but slower table top such as the HexaPOD or highly accurate, fast, but expensive robotic couches. PSS compensation was evaluated for 1D, 2D and 3D motion compensation. 2D dosimetric evaluation confirmed that RMS compensation errors of the order of 1 to 2 mm are not significant and lead to slight smoothing of the dose in the main direction of motion as well as its perpendicular direction. MPC relies on an accurate model of the system; however a linear approximation of the nonlinear PSS can be used within the control algorithm as long as an inversion strategy is adopted to limit the effect of nonlinearities and in particular the dead zone. Issues associated with the inversion technique to cancel out the dead zone should however be considered for commercial implementations. Currently most robotic systems used in medical devices use standard controllers, such as PID, that have been shown to work well in a predictable manner. The use of MPC is believed to be the logical progression for systems which require finding a trade off between achieving both accurate and smooth motion to reduce equipment wear and take into account patient's comfort. MPC offers improved performances for a wider range of operating conditions but at the cost of higher complexity. The later is becoming manageable with current increases in computational power. This has made MPC the 'new PID' in many industries. This paper focused on patient support system; however designing a control system for motion tracking and compensation is equally applicable to MLC or gantry control. The combination of dose rate variation and PSS compensation is promising however further work is required to identify both effective and efficient beam switching strategies.

Acknowledgments

This work was sponsored by the Framework 6 European integrated project Methods and Advanced Equipment for Simulation and Treatment in Radiation Oncology (MAESTRO) CE LSHC CT 2004 503564. The Authors are grateful to the Department of Radiation Oncology, Virginia Commonwealth University, USA for providing some of the data used in this manuscript. The Authors are also grateful to the staff of the Radiotherapy Departments at the University Hospital, Coventry, UK, the Addenbrookes, Western General, Edinburgh UK and the Newcastle General Hospitals, Newcastle, UK for their assistance in realising the measurements presented in this paper.

References

Buzurovic I, Huang K, Yu Y and Podder T K 2011a A robotic approach to 4D real-time tumor tracking for radiotherapy *Phys. Med. Biol.* **56** 5 1299-318

Buzurovic I, Yu Y and Podder T K 2011b Active tracking and dynamic dose delivery for robotic couch in radiation therapy *Engineering in Medicine and Biology Society, EMBC, 2011 Annual International Conference of the IEEE* pp 2156-9

Crijns S P M, Kok J G M, Lagendijk J J W and Raaymakers B W 2011 Towards MRI-guided linear accelerator control: gating on an MRI accelerator *Phys. Med. Biol.* **56** 15 4815

Depuydt, T *et al* 2011 Geometric accuracy of a novel gimbals based radiation therapy tumor tracking system *Radiotherapy and Oncology* **98** 3 365-72

D'Souza W D, Malinowski K T, Van Liew S, D'Souza G, Asbury K, McAvoy T J, Suntharalingam M and Regine W F 2009 Investigation of motion sickness and inertial stability on a moving couch for intra-fraction motion compensation *Acta Oncol.* **48** 8 1198-203

D'Souza W D and McAvoy T J 2006 An analysis of the treatment couch and control system dynamics for respiration-induced motion compensation *Med. Phys.* **33** 12 4701-9

D'Souza W D, Naqvi S A and Yu C X 2005 Real-time intra-fraction-motion tracking using the treatment couch: a feasibility study *Phys. Med. Biol.* **50** 4021-33

dSPACE, G *DS1104 R&D Controller Board* : 2012 dSPACE GmbH

Ernst F, Schlaefer A and Schweikard A 2011 Predicting the outcome of respiratory motion prediction *Med. Phys.* **38** 10 5569-81

George R, Vedam S S, Chung T D, Ramakrishnan V and Keall P J 2005 The Application of the sinusoidal model to lung cancer patient respiratory motion *Med. Phys.* **32** 9 2850-61
Haas O C L, Bueno G, Spriestersbach R, Himmler H, Burnham K J and Mills J A 2005 Imaging and Control for Adaptive Radiotherapy *16th IFAC World Congress, Http://www.Ifac-Papersonline.net/Detailed/29399.Html, 10.3182/20050703-6-CZ-1902.02118* : ELSEVIER)
Haas O C L, Paluszczyszyn D, Ruta M and Skworcow P 2011 Motion prediction and control for patient motion compensation in radiotherapy *18th IFAC World Congress Milano (Italy), Http://www.Ifac-Papersonline.net/Detailed/49451.Html, 10.3182/20110828-6-IT-1002.03559* : The International Federation of Automatic Control (IFAC)) pp 5985-90
Haas O C L 2010a last updated 2 Sep 2010 *Moving the PSS form a computer system* [Homepage of CovStudent], [Online]. Available: http://www.youtube.com/watch?v=wONg0b4t2os&feature=player_embedded [June 2012]
Haas O C L 2010b last updated 15 Mar 2010 *Fighting Cancer with Control Theory* [CovStudent] [Online]. Available: http://www.youtube.com/watch?v=aUVmGoLEpCI&feature=player_embedded [June 2012]
Haas O C L, Burnham K J and Mills J A 1998 Optimization of beam orientation in radiotherapy using planar geometry *Phys. Med. Biol.* **43** 8 2179-93
Han K, Cheung P, Basran P S, Poon I, Yeung L and Lochray F 2011 A comparison of two immobilization systems for stereotactic body radiation therapy of lung tumors *Radiother Oncology* **95** 1 103-8
Herrmann C, Ma L and Schilling L 2011 Model Predictive Control for Tumor Motion Compensation in Robot Assisted Radiotherapy *Proceedings of the 18th IFAC World Congress, 2011* : IFAC)
Hoogeman M, Prévost J B, Nuyttens J, Pöll J, Levendag P and Heijmen, B 2009 Clinical accuracy of the respiratory tumor tracking system of the cyberknife: assessment by analysis of log files *Int. J. Radiat. Oncol. Biol. Phys.* **74** 1 297-303
Jiang S B 2006 Technical aspects of image-guided respiration-gated radiation therapy *Medical Dosimetry* **31** 2 141-51
Kakar M 2010 *Intelligent and Adaptive Systems in Cancer Biomedicine: Methods and Applications* : LAP LAMBERT Academic Publishing
Kamino Y, Takayama K, Kokubo M, Narita Y, Hirai E, Kawawda N, Mizowaki T, Nagata Y, Nishidai T and Hiraoka M 2006 Development of a four-dimensional image-guided radiotherapy system with a gimbaled X-ray head *Int. J. Radiat. Oncol. Biol. Phys.* **66** 1 271-8
Keall P J, Cattell H, Pokhrel D, Dieterich S, Wong K H, Murphy M J, Vedam S S, Wijesooriya K and Mohan R 2006 Geometric accuracy of a real-time target tracking system with dynamic multileaf collimator tracking system *Int. J. Radiat. Oncol. Biol. Phys.* **65** 5 1579-84
Krauss A, Nill S N, Tacke M and Oelfke U 2011 Electromagnetic Real-Time Tumor Position Monitoring and Dynamic Multileaf Collimator Tracking Using a Siemens 160 MLC: Geometric and Dosimetric Accuracy of an Integrated System *International Journal of Radiation Oncology Biology Physics* **79** 2 579-87
Loo H, Fairfoul J, Chakrabarti A, Dean J C, Benson R J, Jefferies S J and Burnet N G 2011 Tumour shrinkage and contour change during radiotherapy increase the dose to organs at risk but not the target volumes for head and neck cancer patients treated on the TomoTherapy HiArt™ system *Clin. Oncol. (R. Coll. Radiol.)* **23** 1 40-7
Maciejowski J M 2002 *Predictive Control with Constraints* : Pearson Education Limited, England) pp 331
MathWorks 2011 *MATLAB and Simulink* : The MathWorks Inc
Murphy M J, Eidens R, Vertatschitsch E and Wright J N 2008 The Effect of Transponder Motion on the Accuracy of the Calypso Electromagnetic Localization System *International Journal of Radiation Oncology Biology Physics* **72** 1 295-9
Murphy M J and Pokhrel D 2009 Optimization of an adaptive neural network to predict breathing *Med. Phys.* **36** 1 40-7
Popple R A and Brezovich I A 2011 Dynamic MLC leaf sequencing for integrated linear accelerator control systems *Med. Phys.* **38** 11 6039-45

Putra D, Haas O C L, Mills J A and Burnham K J 2008 A multiple model approach to respiratory motion prediction for real-time IGRT *Phys. Med. Biol.* **53** 6 1651-563

Putra D, Skworcow P, Haas O C L, Burnham K J and Mills J A 2007 Output-Feedback Tracking for Tumour Motion Compensation in Adaptive Radiotherapy *American Control Conference, 2007. ACC '07* pp 3414-9

Qiu P, 'D'Souza W, McAvoy T and Ray Liu K 2007 Inferential modeling and predictive feedback control in real-time motion compensation using the treatment couch during radiotherapy.*Phys. Med. Biol.* **52** 19 5831-54

Rijkhorst E, Lakeman A, Nijkamp J, de Bois J, van Herk M, Lebesque J V and Sonke J 2009 Strategies for Online Organ Motion Correction for Intensity-Modulated Radiotherapy of Prostate Cancer: Prostate, Rectum, and Bladder Dose Effects *International Journal of Radiation Oncology Biology Physics* **75** 4 1254-60

Sahih A 2010 Respiratory Motion Modelling and Predictive Tracking for Adaptive Radiotherapy Coventry University

Skworcow P 2008 Modelling and predictive control of radiotheraphy treatment machines Coventry University

Skworcow P, Putra D, Sahih A, Goodband J, Burnham K J, Haas O C L and Mills J A 2007 Predictive Tracking for Respiratory Induced Motion Compensation in Adaptive Radiotherapy *Measurement + Control* **40** 1 16-9

Sun B, Rangaraj D, Papiez L, Oddiraju S, Yang D and Li H H 2010 Target tracking using DMLC for volumetric modulated arc therapy: a simulation study *Med. Phys.* **37** 12 6116-24

Tacke M B, Nill S, Krauss A and Oelfke U 2010 Real-time tumor tracking: automatic compensation of target motion using the Siemens 160 MLC *Med. Phys.* **37** 2

Trofimov A, Vrancic C, Chan T C Y, Sharp G C and Bortfeld T 2008 Tumor trailing startegy for intensity-modulated radiation therapy of moving targets *Med. Phys.* **35** 1718-33

Verellen, D, Ridder, M D and Storme, G 2008 A (short) history of image-guided radiotherapy *Radiotherapy and Oncology* **86** 1 4-13

Wong J W, Sharpe M B, Jaffray D A, Kini V R, Rovertson J M, Stromberg J S and Martinez A A 1999 The use of active breathing control (ABC) to reduce margin for breathing motion *Int.J.Radiation Oncology Biol.Phys.* **44** 4 911-9

Woo M K and Kim B 2002 An investigation of the reproducibility and usefulness of automatic couch motion in complex radiation therapy techniques *J Appl Clin Med Phys* **3** 1 46-50

Yang W, Jones R, Read P, Benedict S and Sheng K 2011 Standardized evaluation of simultaneous integrated boost plans on volumetric modulated arc therapy *Phys. Med. Biol.* **56** 2 327-39